

Lasers in Manufacturing Conference 2019

# Application of different pulsed laser sources to dissimilar welding of Cu and Al alloys

Alessandro Ascari<sup>a\*</sup>, Alessandro Fortunato<sup>a</sup>, Erica Liverani<sup>a</sup>, Adrian Lutey<sup>b</sup>

<sup>a</sup>University of Bologna, Viale Risorgimento 2, 40136, Bologna, Italy

<sup>b</sup>University of Parma, Via delle Scienze 181/a, 43124, Parma, Italy

---

## Abstract

The paper deals with laser dissimilar welding of aluminum and copper alloys thin sheets. In particular, the application of different laser sources was investigated, both in terms of general applicability and of weld bead characteristics. The lap welding configuration considered in the experiments was Al over Cu, in order to evaluate the role of the material combination with respect to the laser radiation and to the formation of different compounds in the fused zone. The laser sources exploited were chosen among pulsed wave ones and in particular: high brilliance quasi-CW fiber source, low brilliance long-pulse lamp-pumped Nd:YAG one and high brilliance short-pulse Q-switched fiber one. The results were characterized by means of tensile tests, in order to understand the mechanical characteristics of the weldments and by means of metallographic techniques, in order to understand the metallurgical properties.

Keywords: Pulsed-wave; Dissimilar welding; High-reflectivity; Lap-welding.

---

## 1. Introduction

Autogenous welding of dissimilar metals, such as aluminum and copper, is very challenging for several reasons. First of all, copper and aluminum, after re-solidification, tend to form intermetallic compounds which are always hard and brittle and which cause embrittlement of the whole joint, as shown in Zuo et al., 2014 and in Kalaiselvan et al., 2014. Furthermore, these materials show very different chemical and physical properties, such as melting temperature, thermal conductivity and coefficient of thermal expansion, which cause uneven temperature and stress distributions and consequent different thermal deformations and increasing fragility of the joint. For these reasons, many researchers have proposed, over the years, different

---

\* Corresponding author. Tel.: +39-051-2090494.  
E-mail address: a.ascari@unibo.it.

solutions for aluminum-copper welding, with the goal of limiting dilution of the two elements and thermal deformations: for these reasons the most investigated technologies were brazing and welding with filler wire, as shown in Panaskar et al., 2017, Meshram et al., 2007, Saeid et al., 2010, Feng et al., 2012 and Solchenbach et al., 2013. However, the use of those welding technologies is not suitable for many industrial fields where mass production and/or miniaturization are requested. In order to overcome these limitations, several researchers have proposed the use of laser sources, which have the advantage of being very flexible in terms of weldable joint geometries and allow high process speed, too. Moreover, the continuous progress in laser sources manufacturing allow to effectively deal with the high reflectivity typical of both copper and aluminum reducing, at the same time, the amount of heat delivered to target workpiece. In this direction Lee, et al., 2014 reported that laser can improve Cu-Al welding by reducing the solidification time which leads to a minimum quantity of intermetallic compounds formation, that are the main drawbacks in this technology, as shown also in Kah et al., 2015 and Lee et al., 2005. Autogenous laser welding of Al-Cu and Cu-Al, minimizing the heating of the thin sheets, have been successfully reported in several other researches, as shown in Mai et al., 2004 and Fetzer et al., 2016. Considering the above-mentioned results, this paper gives an overview of the application of three different pulsed sources currently available on the market: a high brilliance and a low brilliance long pulsed ones and a short pulse high brilliance one. This investigation allows to understand the role of different spot dimensions and different temporal distributions of the radiation given a specific welding configuration (lap welding of aluminum on copper) and two fixed materials with a definite thickness (0.4 mm thick pure aluminum and 0.3 mm thick pure copper). The results were analyzed in terms of weld bead morphology, eventual defects and mechanical performance.

## 2. Experimental Setup

All the experiments were carried out on pure copper (Cu > 99.6%), covered by a nickel layer to improve optical absorptivity, and commercially aluminum AA1060 (99.4% Al, 0.25% Si and 0.35% Fe). The samples size was 80x45 mm, while the thickness was 0.3 mm for the copper sheet and 0.4 mm for the aluminum one. The joint configuration is shown in Fig. 1: the overlapping region of the sheets was 15 mm wide and the weld bead was carried out in the middle of it. Fig. 2 explains the measure geometrical parameters, while the physical, chemical and optical properties of the two materials are reported in Table 1.

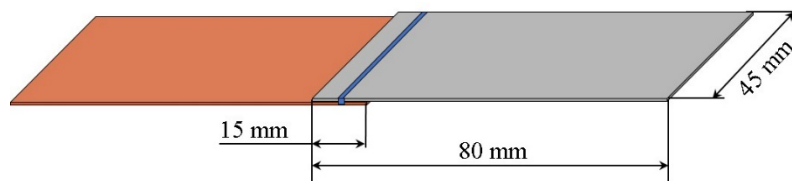


Fig. 1. Joint configuration

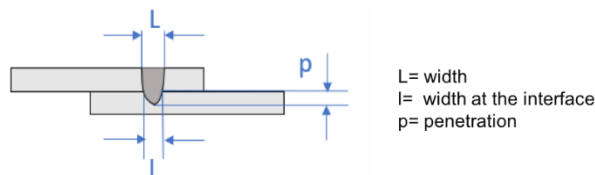


Fig. 2. Weld bead morphological characteristics

Table 1. Physical characteristics of the welded materials

	Copper	Aluminum
Density [g/cm <sup>3</sup> ]	8.9	2.71
Melting temperature [°C]	1083	660
Thermal conductivity [W/(m·K)]	390	660
Thermal expansion coefficient [°C <sup>-1</sup> ]	17·10 <sup>-6</sup>	24·10 <sup>-6</sup>
Specific heat capacity [J/(kg·K)]	385	880
Absorptivity @1064 nm	2-3%	5-7%

The main characteristics of the laser sources exploited are reported in Table 2: they were characterized by very different characteristics, especially in terms of spot dimensions and of temporal profiles of the radiation. Those sources allowed a wide range of power densities on the workpiece: from approximately 600 MW/cm<sup>2</sup> of the high brilliance short pulse one to 0.06 MW/cm<sup>2</sup> of the low brilliance long pulse one.

Table 2. Laser equipment exploited

	IPG YLR 300-3000 QCW	Trumpf HL-204P	SPI G4 EP-Z 100W
Mode	Long pulse	Long pulse	Short pulse
Max. average power [W]	300	200	100
Max peak power [kW]	3	7	10
Max. pulse energy [J]	30	75	0.001
Pulse duration	0.1-50 ms	0.5-20 ms	17-320 ns
Max. pulse frequency [kHz]	5	0.6	2000
BPP [mm·mrad]	2	16	0.54
Fiber core diameter [μm]	50	400	n/a
Focal length [mm]	90	135	160
Spot diameter [μm]	75	635	46
Maximum power density [MW/cm <sup>2</sup> ]	6.8	0.063	5.9
Maximum peak power density [MW/cm <sup>2</sup> ]	67.9	2.2	595.5
Focusing head	Fixed focal	Galvo	Galvo

### 3. Results and Discussion

#### 3.1 Welding with IPG YLR 300-3000 QCW

The experiments involving the IPG YLR 300-3000 QCW were carried out in two sequential steps: a first explorative one and a fine tuning one. The first step was devoted to understanding a rough process window: in this case several pulse durations were tested, from 5 ms to 0.1 ms and the results pointed out that high values of this parameter determine a consequentially high energy per pulse. The high reflectivity of the involved materials, in fact, asks for a relatively high peak power (at least 600 W according to the experiments) in order to trigger the formation of the keyhole and properly melt the metal layers: this implies a high energy per pulse if the pulse duration increases. This situation leads to two negative effects: a high

heat input in the material and a low pulse frequency and thus a low welding speed, given the maximum average power of 300 W. Considering these conditions the best trade-off in terms pulse duration turned to be the value of 0.1 ms. In Table 3 the main process parameters characterizing the experimental campaign are shown.

Table 3. Experimental parameters (IPG YLR 300-3000 QCW)

Average power [W]	Peak power [W]	Pulse duration [ms]	Pulse energy [J]	Pulse frequency [Hz]	Pulse overlap [%]	Speed [mm/s]	Heat input [J/mm]
300	1000	0.1	0.1	3000	85	33.8	8.9
300	1100	0.1	0.11	2727	85	30.7	9.8
300	1200	0.1	0.12	2500	85	28.1	10.7
300	1300	0.1	0.13	2308	85	26.1	11.6
300	1400	0.1	0.14	2143	85	24.1	12.5
300	1500	0.1	0.15	2000	85	22.5	13.3
300	1600	0.1	0.16	1876	85	21.1	14.2
300	1700	0.1	0.17	1768	85	19.6	15.1

The graph in Fig. 3 shows the results in terms of weld bead penetration and weld bead width at the interface between the sheets.

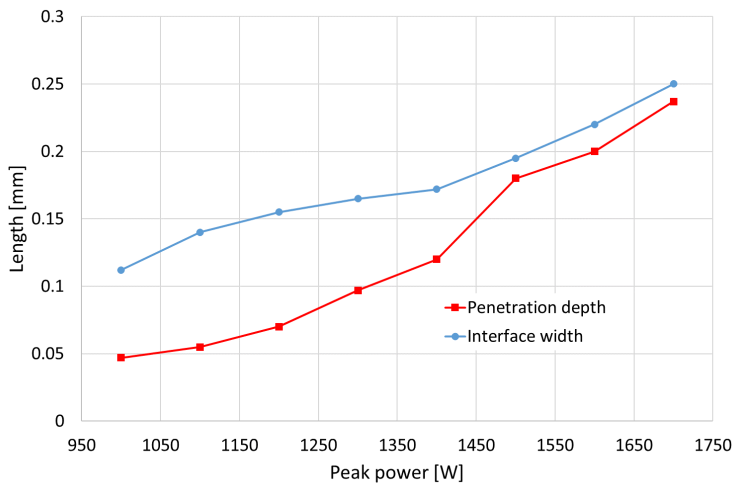


Fig. 3. Weld bead penetration and width at the interface (IPG YLR 300-3000 QCW)

It is clear that both parameters are directly proportional to peak power and their values can be finely tuned acting on the peak power itself. The maximum value of 1700 W was not exceeded in the experiments because of the fact that full penetration in the copper layer had to be avoided. Fig. 4 shows three examples of weld bead characterized by maximum, average and minimum penetration, respectively. The micrographs point out that the average quality of the weldments is good and no porosity or crack were formed. Only the weld bead obtained with the maximum peak power shows evident undercut and irregular top surface. The

specimens were subjected to shear test by means of an Instron 8032 machine equipped with a 1 kN load cell and a traverse speed equal to 0.025 mm/s. Fig. 5 shows the maximum loads registered for every specimen: it is clear that there is an optimum peak power between 1300 W and 1500 W, which leads to the best mechanical resistance of the weld bead. For lower peak powers, in fact, the fusion zone is small and the width at the interface does not guarantee sufficient resistance area, while for higher powers the weld bead face is irregular and prone to undercuts and the high dilution between copper and aluminum promotes the formation of fragile intermetallic compounds, leading to a less performing joint.

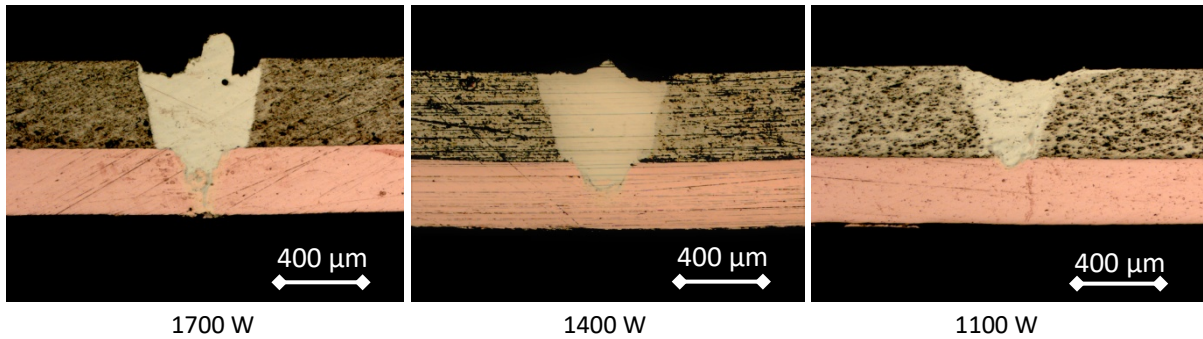


Fig. 4. Examples of weld beads (IPG YLR 300-3000 QCW)

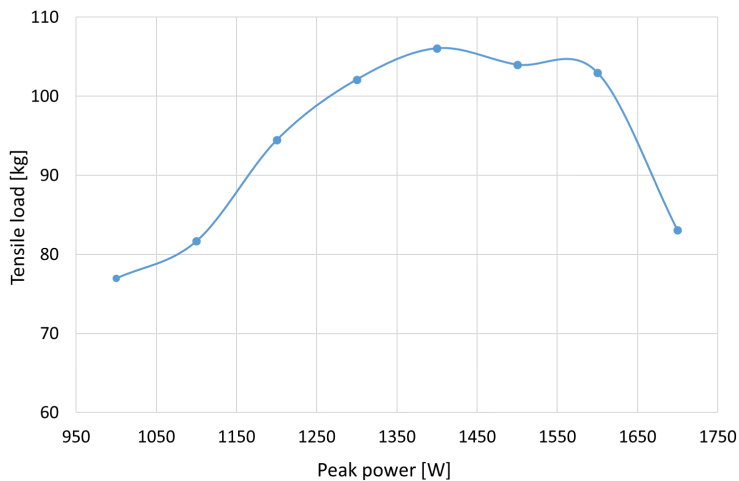


Fig. 5. Tensile tests results (IPG YLR 300-3000 QCW)

### 3.2 Welding with Trumpf HL-204P

Also in this case a rough process window was determined by means of a preliminary experimental campaign and the results reported herein concern the fine-tuning phase. The much larger spot typical of this source forced a completely different approach to the experiments: the peak power was set constant to 6000 W and the pulse duration was tuned in order to understand its effects on the weld bead. Table 4 shows the process parameters exploited. The graph in Fig. 6 shows the results in terms of weld bead penetration and

weld bead width at the interface between the sheets. It is clear that both parameters are directly proportional to pulse duration, but the low brilliance characteristic of the laser source did not allow to fine tune them acting on pulse duration itself. In particular the control of penetration depth was quite difficult: for pulse durations lower than 2 ms no welding occurred, while for values larger than 4 ms full penetration occurred and all the thickness of the copper layer was affected by melting. The graph shows also a great difference in the average dimensions of the weld bead compared to the previous ones: in this case the width, in particular, is much larger than the one measured in case of higher brilliance sources.

Table 4. Experimental parameters (Trumpf HL-204P)

Average power [W]	Peak power [W]	Pulse duration [ms]	Pulse energy [J]	Pulse frequency [Hz]	Pulse overlap [%]	Speed [mm/s]	Heat input [J/mm]
200	6000	2.0	12	17	50	5.4	36.9
200	6000	3.0	18	11	50	3.6	55.4
200	6000	4.0	24	8	50	2.7	73.8
200	6000	6.0	36	6	50	1.8	110.8

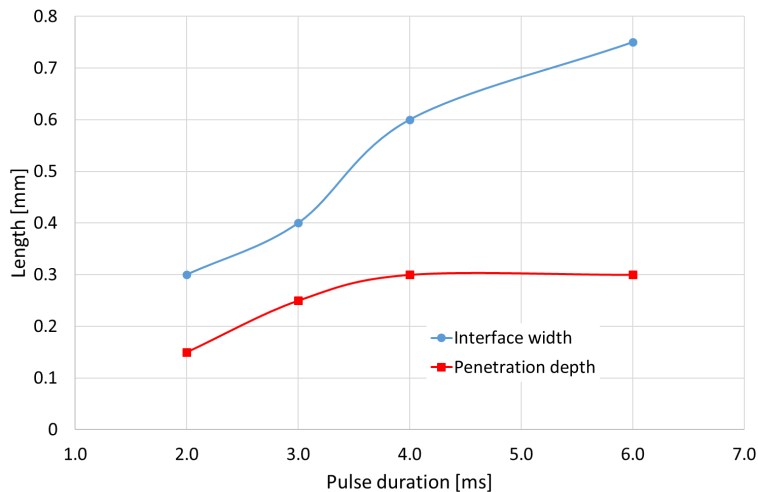


Fig. 6. Weld bead penetration and width at the interface (Trumpf HL-204P)

Fig. 7 shows some examples of weld bead characterized by different penetration depths and widths as a function of the pulse duration. The micrographs point out that the average quality of the weldments is fair, since for high pulse duration several porosities show up. The specimens were subjected to shear test by means of an Instron 8032 machine equipped with a 1 kN load cell and a traverse speed equal to 0.025 mm/s. Fig. 8 shows the maximum loads registered for every specimen: it is clear that there is an optimum pulse duration at about 3 ms which leads to the best mechanical resistance of the weld bead. For lower durations, in fact, the fusion zone is small and the width at the interface does not guarantee sufficient resistance area, while for higher ones the high dilution between copper and aluminum promotes the formation of fragile intermetallic compounds and the porosities increase.

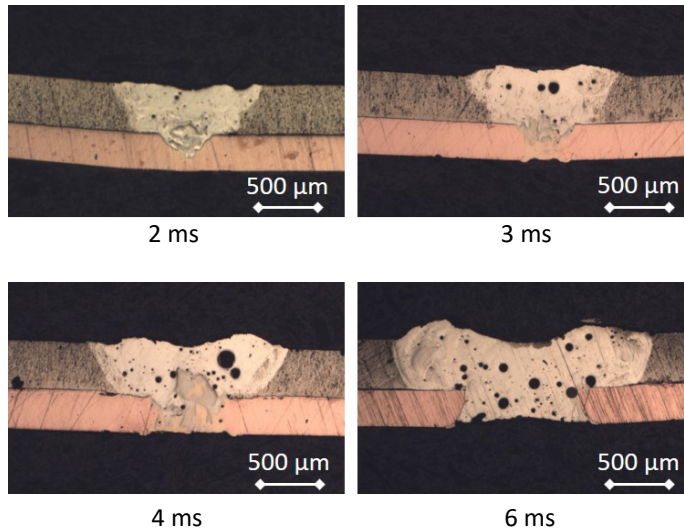


Fig. 7. Examples of weld beads (Trumpf HL-204P)

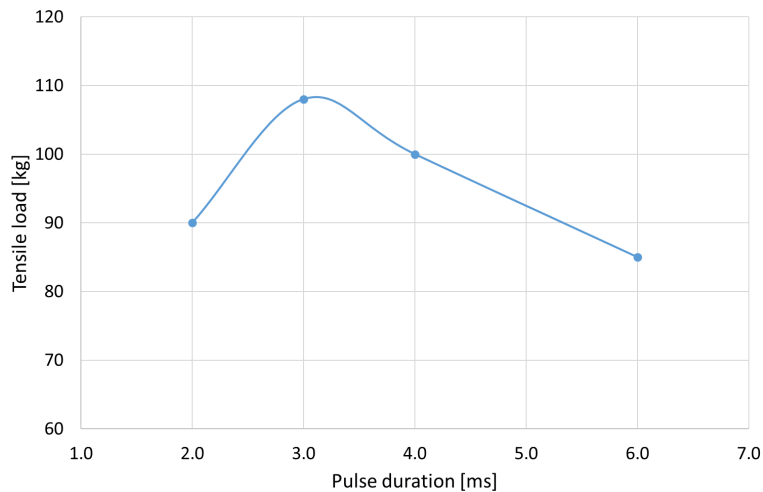


Fig. 8. Shear tests results (Trumpf HL-204P)

### 3.3 Welding with SPI G4 EP-Z 100W

Also in this case a rough process window was determined by means of a preliminary experimental campaign and the results reported herein concern the fine-tuning phase. The very small spot and the high power density per pulse typical of this source determined the need of exploiting a wobbling technique in order to enlarge the melt pool and to make the weld bead face more stable and less humpy and irregular. Among the different waveforms typical of this source the WFO was chosen, which is characterized by the parameters reported in Table 5. The best results were obtained exploiting the parameters reported in Table 6.

Table 5. Characteristic parameters of the chosen waveform (SPI G4 EP-Z 100W)

Nominal frequency [kHz]	Maximum frequency [kHz]	Pulse duration [ms]	Max. pulse energy [mJ]	FWHM pulse width @ max. energy [ns]	Pulse width @ 10% [ns]	Peak power @ max. energy [kW]
100	2000	2.0	1	50	280	10

Table 6. Experimental parameters (SPI G4 EP-Z 100W)

Average power [W]	Peak power [kW]	Pulse frequency [kHz]	Pulse energy [mJ]	Wobbling width [mm]	Wobbling frequency [Hz]	Speed [mm/s]	Heat input [J/mm]
100	10	100	1	0.1	500	12.5	8
100	10	200	0.5	0.1	500	12.5	8
100	10	300	0.33	0.1	500	12.5	8
100	10	400	0.25	0.1	500	12.5	8
100	10	500	0.2	0.1	500	12.5	8

The graph in Fig. 9 shows the results in terms of weld bead penetration and weld bead width at the interface between the sheets. In this case the high energy per pulse associated to the low frequencies determines a high penetration depth and a small width: the optimum trade-off between depth and width is obtained for a pulse repetition rate equal to 300 kHz, where the width at the interface is the highest one and the penetration depth is not very high and thus the dilution between the two parent metals is limited.

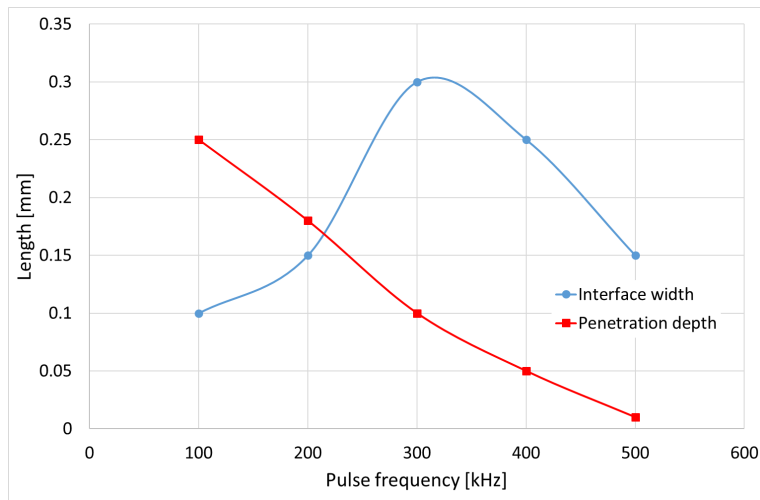


Fig. 9. Weld bead penetration and width at the interface (SPI G4 EP-Z 100W)



This behavior is also underlined by the micrographs in Fig. 10. The specimens were subjected to shear test by means of an Instron 8032 machine equipped with a 1 kN load cell and a traverse speed equal to 0.025 mm/s. Fig. 11 shows the maximum loads registered for every specimen: it is clear that there is an optimum pulse frequency at about 300 kHz which leads to the best mechanical resistance of the weld bead. For lower frequencies, in fact, the width at the interface does not guarantee sufficient resistance area and the high penetration determines a high dilution of the parent materials and thus promotes the formation of brittle intermetallic phases, while for higher ones the width at the interface is once again small.

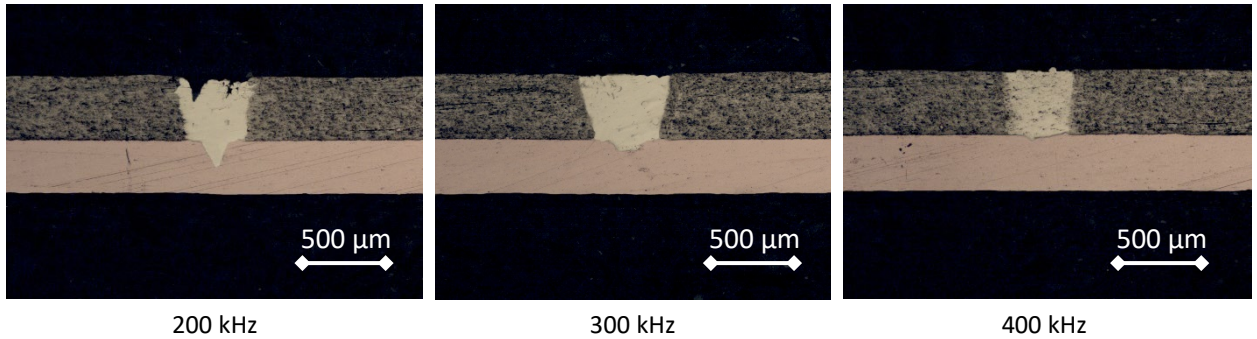


Fig. 10. Examples of weld beads (SPI G4 EP-Z 100W)

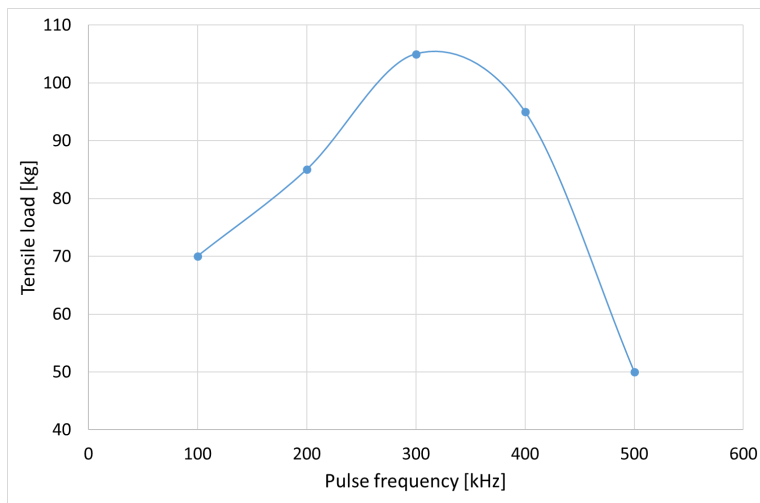


Fig. 11. Shear test results (SPI G4 EP-Z 100W)

#### 4. Conclusions

The paper deals with laser lap welding of aluminum and copper thin sheets in dissimilar configuration. Three different pulsed laser sources with different beam quality and temporal profile were exploited in order to understand the feasibility of the process. The test results underlined the following considerations:

- Given the high reflectivity and high thermal conductivity of the base materials, an important role is played by the spot dimension: a smaller one favors much wider process windows and a more robust process control.
- Both long and short pulse sources turned to be applicable and allowed to achieve very interesting results, both in terms of bead quality and of productivity.
- Weld bead mechanical resistance strictly depends on weld bead dimensions but also on its metallurgical characteristics: too high heat inputs promote a larger dilution of the parent metals, determining the formation of fragile intermetallic phases.

#### References

- Feng, J., Songbai, X., Wei, D., 2012. Reliability studies of Cu/Al joints brazed with Zn–Al–Ce filler metals. *Materials & Design* 42, p. 156-163.
- Fetzer, F., Jarwitz, M., Stritt, P., Weber, R., Graf, T., 2016. Fine-tuned Remote Laser Welding of Aluminum to Copper with Local Beam Oscillation. *Physics Procedia* 83, p. 455-462.
- Kah, P., Vimalraj, C., Martikainen, J., Suoranta, R., 2015. Factors influencing Al-Cu weld properties by intermetallic compound formation. *International Journal of Mechanical and Materials Engineering* 10, p. 10.
- Kalaiselvan, K., Elango, A., 2014. Studies of Interfacial Microstructure and Mechanical Properties on Dissimilar Sheet Metal Combination Joints Using Laser Beam Welding. *International Journal of Mechanical, Aerospace, Industrial, Mechatronic and Manufacturing Engineering* 8(11), p. 1903-1911.
- Lee, S.J., Nakamura, H., Kawahito, Y., Katayama, S., 2014. Effect of welding speed on microstructural and mechanical properties of laser lap weld joints in dissimilar Al and Cu sheets. *Science and Technology of Welding and Joining* 19(2), p. 111-118.
- Lee, W.B., Bang, K.S., Jung, S.B., 2005. Effects of intermetallic compound on the electrical and mechanical properties of friction welded Cu/Al bimetallic joints during annealing. *Journal of Alloys and Compounds* 390, p. 212-219.
- Mai, T.A., Spowage, A.C., 2004. Characterisation of dissimilar joints in laser welding of steel–kovar, copper–steel and copper–aluminium. *Materials Science and Engineering A* 374(1-2), p. 224-233.
- Meshram, S.D., Mohandas, T., Reddy, G.M., 2007. Friction welding of dissimilar pure metals. *Journal of Materials Processing Technology* 184, p. 330-337.
- Panaskar, N., Terkar, R., 2017. A Review on Recent Advances in Friction Stir Lap Welding of Aluminium and Copper. *Materials Today* 4(8), p. 8387-8393.
- Saeid, T., Abdollah-Zadeh, A., Sazgari, B., 2010. Weldability and mechanical properties of dissimilar aluminium–copper lap joints made by friction stir welding. *Journal of Alloys and Compounds* 490, p. 652–655.
- Solchenbach, J., Plapper, P., 2013. Mechanical characteristics of laser braze-welded aluminium–copper connections. *Optics & Laser Technology* 54, p. 249-256.
- Zuo, D., Hu, S., Shen, J., Xue, Z., 2014. Intermediate layer characterization and fracture behavior of laser-welded copper/aluminum metal joints. *Materials and Design* 58, p. 357-362.